PHYSICAL REVIEW B VOLUME 41, NUMBER 8 15 MARCH 1990-I

Abrupt interfaces with novel structural and electronic properties: Metal-cluster deposition and metal-semiconductor junctions

G. D. Waddill, I. M. Vitomirov, C. M. Aldao, S. G. Anderson, C. Capasso, and J. H. Weaver
Department of Chemical Engineering and Materials Science, University of Minnesota, Minneapolis, Minnesota 55455

Z. Liliental-Weber
Lawrence Berkeley Laboratory, Berkeley, California 94720
(Received 11 September 1989)

Abrupt interfaces with no observed substrate disruption are produced by a novel method of metal-semiconductor junction formation. This method involves the condensation of a thin Xe buffer layer on cleaved surfaces to isolate the semiconductor from impinging metal atoms. This Xe buffer layer provides a surface upon which the metal atoms diffuse, nucleate, and grow into metallic clusters. These clusters are then brought into contact with the substrate when the Xe is thermally desorbed. The result is an abrupt, nondisrupted, nearly ideal interface. Photoemission studies of Al, Ag, Au, Ga, Ti, and Co clusters grown on *n*- and *p*-type GaAs(110) show unique Fermi-level positions ~0.3 and 1.0 eV below the conduction-band minimum, respectively, that are nearly metal and coverage independent. We find no evidence that metal-induced gap states or conventional defect levels are important in determining the Fermi-level position in the gap, but photoemission results indicate surface unrelaxation around the clusters. This unrelaxation results in the reappearance of states in the gap. High-resolution electron-microscopy results for Au(clusters)/GaAs(110) show intimate contact with no intermixing at the interface, with sintering of Au clusters to form an interconnected network of metal islands at high coverages. Comparisons of these results with those for interfaces formed by atom deposition at 60 and 300 K emphasize the novel properties of the cluster interface.

INTRODUCTION

Studies of Schottky-barrier formation at metal-semiconductor interfaces have been complicated by the difficulty of producing an abrupt, "ideal" interface. The commonly used methods of producing metal-semiconductor interfaces result in complex interface morphologies, including substrate disruption, atomic interdiffusion, alloy or compound formation, and structural changes of the substrate surface. The complicated nature of such interfaces makes it difficult, from a fundamental point of view, to identify the mechanism(s) dominating Schottky-barrier (SB) formation for the various stages of its development.

A number of models have been proposed to explain SB formation at interfaces grown by atom-by-atom deposition techniques. They include models based on adsorption-induced defect formation,[1] interface chemistry,[2] effective work function,[3] metal-induced gap states (MIGS),[4] and bulk-semiconductor crystal quality.[5] Recently, a number of studies of SB formation at low temperature (60–200 K) were performed in an attempt to inhibit certain interfacial interactions and thereby exclude their effect on SB formation.[6–9] These studies established that metal clustering and atomic interdiffusion were reduced at low temperature, while demonstrating that adatom-induced substrate disruption was effectively independent of temperature.[8,9] The primary difference between interfaces formed at 60 and 300 K was found to involve the distribution of the liberated substrate atoms in the evolving interface. This redistribution was kinetically limited with released substrate atoms trapped near the interface at 60 K, but diffused toward the vacuum interface at 300 K. These studies also revealed temperature- and dopant-concentration-dependent SB evolution which cannot be explained with existing models. It has been successfully interpreted in terms of a dynamic coupling model (DCM) which accounts for the coupling between the bulk semiconductor and the metal-induced surface states through the surface-depletion region.[10]

To create "ideal" boundary regions, we have developed a method of joining preformed metal clusters with atomically clean semiconductor surfaces.[9] Our approach has been to isolate the substrate from the impinging metal-atom flux and thereby avoid complexity at the surface due to adatom impact and bonding. In this way it is possible to prevent adatoms from interacting with the surface until they have agglomerated into clusters. To achieve this, we first condense a thin layer of solid Xe on the clean substrate at 60 K and then deposit metal atoms onto this buffer layer. Adatom mobility is sufficient to assure the formation of metallic clusters on and within the Xe. These clusters come into contact with the clean surface when the Xe buffer is thermally desorbed.

In this paper we show that metal-GaAs(110) interfaces formed by cluster deposition display unique band bending, with E_F positions that are largely metal independent for *n*-type GaAs, but more dependent on the metal for *p*-type GaAs. Results for M/GaAs interfaces, where M

 © 1990 The American Physical Society

denotes Ag, Al, Au, Co, Ga, and Ti, are presented. These metals were chosen because they were known to exhibit a variety of interfacial interactions for atom deposition and, consequently, presented the possibility of presenting a variety of behaviors upon clustering and subsequent deposition. In particular, Ag and Ga both cluster spontaneously upon atom deposition at 300 K and it was possible to directly compare band bending for systems which were expected to have the same final morphology. Titanium was chosen because it is a highly reactive refractory metal. Cobalt is less reactive than Ti, and aluminum induces exchange reactions with Ga at the Al/GaAs interface at room temperature. In addition, these metals exhibit a very wide range of melting temperatures, so that effects related to sintering or wetting might be expected.

The results presented here show changes in E_F position that reflect a balance between the dopant concentration and the intercluster separation for heavily doped p-type GaAs, with uniform pinning observed when the average cluster spacing is less than the Debye length. Significantly, there is no evidence for MIGS or conventional adatom-induced defect levels near midgap. Detailed analysis of substrate core-level spectra shows that cluster deposition produces a defect-free boundary for GaAs(110), and quantitative analysis shows that the attenuation of the surface-shifted component is consistent with surface unrelaxation around the clusters. Temperature-dependent studies in the 60–300-K range for cluster/GaAs interfaces show interface stability in all cases except Ti, where warming to 300 K led to metal-substrate reaction and Fermi-level movement toward midgap. High-resolution electron-microscopy results for the Au(cluster)/GaAs(110) interface show an abrupt interface with no evidence for disruption or atomic intermixing. They also show that cluster sintering has occurred during the deposition process, with clear evidence for grain-boundary formation in the composite. No preferred orientation of the Au overlayer structure relative to the GaAs surface is observed. These results for cluster deposition are compared with those for interfaces grown by atom-by-atom deposition which exhibit diverse and metal-dependent interfacial interactions. Finally, early results for InP(110) surfaces show reduction, but not elimination, of reaction between the surface and the cluster.

EXPERIMENTAL PROCEDURES

Synchrotron-radiation photoemission measurements were performed at the Aladdin-electron-storage ring at the University of Wisconsin Synchrotron Radiation Center using the facility's Grasshopper beamlines and the Minnesota–Argonne–Los Alamos Extended Range Grasshopper beamline. Core-level energy-distribution curves (EDC's) were collected using a double-pass cylindrical mirror analyzer in an ultrahigh-vacuum system (base pressure $\sim 5\times10^{-11}$ Torr) described in detail elsewhere.[8] Overall instrumental resolution for Ga and As 3d core-level spectra was maintained at $\sim$200 and $\sim$250 meV, respectively. Photon energies of 36 and 65 eV for Ga 3d and 58 and 90 eV for As 3d were used in order to vary the probe depth (3 times the photoelectron mean free path) from $\sim$11 to $\sim$21 Å. Analysis of the EDC's was done using a nonlinear least-squares-minimization curve-fitting routine.[11]

Clean n-type (Si-doped at 1×10^{17} cm^{-3}) and p-type (Zn-doped at 2×10^{18} and 1×10^{17} cm^{-3}) GaAs(110) surfaces were prepared by *in situ* cleaving of $(20\times4\times4)$-mm^3 posts. Mirrorlike cleaves were routinely obtained, and the surface quality was further assessed using core-level and valence-band spectra. Cleaves for which E_F deviated by more than 60 meV from the valence-band maximum (VBM) or conduction-band minimum (CBM) were discarded due to initial partial pinning of the surfaces. Comparisons of core-level photoelectron kinetic energies for n- and p-type GaAs at 60 K showed differences of ≥ 1.42 eV at 60 K, verifying that the clean surfaces were unpinned ($E_g = 1.52$ eV at 60 K).

Metals were evaporated from resistively heated tungsten boats located $\sim$35 cm from the sample surface. Stable evaporation rates, as monitored with a calibrated quartz-crystal microbalance located near the sample, were established prior to exposing the sample to the evaporant. During this procedure, the system pressure did not exceed 4×10^{-10} Torr. Adatom exposures are expressed in Å but uniform surface coverages are not implied.

Sample temperatures of 60 K were achieved by attaching the sample to a copper cold finger mounted on the second stage of a closed-cycle He refrigerator. The temperature was monitored with a Si diode attached to the cold finger, and calibration tests established that the sample temperature was within 5 K of the temperature measured at the diode. Prior to metal deposition, 200 L of Xe [1 langmuir (L) $\equiv 10^{-6}$ Torr s] were condensed on the GaAs(110) surface to produce $\sim$30-Å-thick buffer layers. No measurable changes in sample temperature were observed during metal deposition. It should be noted that each metal-cluster deposition began with a clean, freshly cleaved surface. As detailed in the following, photoemission measurements showed that Xe adsorption and desorption from GaAs(110) did not result in band-bending changes or substrate modification. After cluster formation, the sample was detached from the Cu cold finger and allowed to warm to 300 K. Refrigerator operation was maintained throughout the experiments to minimize the desorption of condensed gas from cold surfaces other than the sample. A turbomolecular pump mounted directly on the chamber provided rapid return to operating pressures. Substrate core-level EDC's were obtained following Xe desorption for sample temperatures over the range $\sim$100–300 K. With the exception of Ti/GaAs, the interfaces formed in this manner were stable.

Following photoemission studies, a sample onto which 7 Å of Au had been deposited by the cluster technique was investigated with scanning electron microscopy to more directly assess the surface coverage and morphology. More detailed insight into the structure at the interface was obtained with transmission electron microscopy

and lattice imaging. As will be discussed, the results showed connected clusters with a nominal thickness of ~60 Å and a lateral dimension of several hundred Å in abrupt contact with the surface.

RESULTS AND DISCUSSION

Xe interactions with GaAs(110)

Figure 1 shows Xe $4d$ EDC's taken at $h\nu=90$ eV for increasing exposures on GaAs(110). Analogous results have been obtained for Xe condensed on InP(110). The binding energies are referenced to the vacuum level of the Xe-covered substrate. For ≤ 10 L, we observe sharp features corresponding to the spin-orbit-split Xe $4d_{3/2}$ and $4d_{5/2}$ levels at 66.5 and 68.5 eV due to the initial monolayer of physisorbed Xe. Increasing the exposure to 10–20 L results in the appearance of a second doublet shifted to higher binding energy that indicates the growth of a second Xe layer. Further exposure to ≥ 40 L reduces the initial monolayer doublet to shoulders on the low-binding-energy side of a broader doublet which arises from emission from condensed Xe multilayers. By 100 L, emission from the first Xe layer is largely attenuated, and the Xe $4d$ line shape remains unchanged after ~500 L. During this growth process, the centroids of the Xe $4d$ levels move to progressively higher binding energy. Equivalent results have been reported by Chiang *et al.*[12] for Xe adsorption on Pd and Al. The energy changes were attributed to differences in final-state screening of Xe $4d$ core holes for atoms close to the substrate compared to those in solid Xe. For Xe/GaAs(110) we find that, as expected for weak Xe-substrate interactions, the monolayer binding energies differ from those reported for Xe/Pd(111) by approximately the difference in the work function of Pd(111) and the electron affinity of GaAs(110).

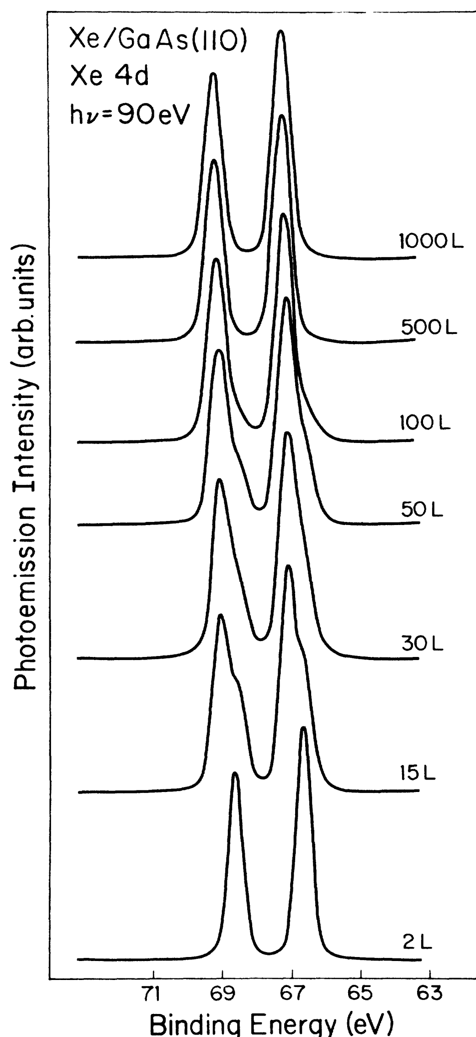

FIG. 1. Xe $4d$ core-level EDC's following adsorption of increasing amounts of Xe on GaAs(110). For ≤ 10 L exposure, the sharp features correspond to the initial monolayer of physisorbed Xe. The shifted doublet for 10–20 L indicates condensation of a second layer. The emission from the first few layers can no longer be distinguished by 500 L, and spectra correspond to those of a thick film.

For our studies of metal-cluster deposition, we chose a Xe coverage of 200 L. From Fig. 1, this is well into the Xe-multilayer regime, and estimates based on GaAs core-level attenuation by the Xe multilayers [using published values of the photoelectron mean free path in Xe (Ref. 13)] indicate the Xe layer to be ~30 Å thick. This was sufficient to minimize interaction of the deposited atoms with the substrate prior to Xe desorption.

In preparation for the metal-cluster experiments, we confirmed that the properties of the GaAs substrate were

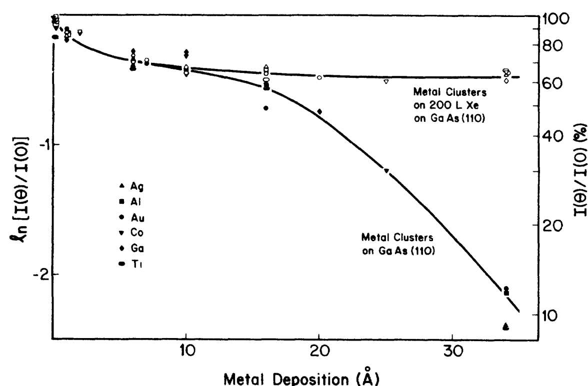

FIG. 2. Upper curve with open symbols shows the rate of attenuation of emission from Xe $4d$ core levels caused by spontaneous metal-cluster growth on 200 L Xe on GaAs(110). Cluster growth produces equivalent attenuation for all of these metals, indicating analogous surface morphologies. Lower curve with solid symbols shows the GaAs substrate attenuation observed when the Xe buffer layer is desorbed and the clusters cover the substrate. For depositions below 10 Å, the clusters are equally effective at covering the Xe layer and, subsequently, the GaAs surface; the rate of attenuation is slow because the clusters leave large exposed regions of the Xe interlayer or the GaAs substrate. For depositions above 10 Å, the faster rate of attenuation for the cluster/GaAs interface suggests cluster coalescence to large two-dimensional islands which occurs during the Xe desorption.

not modified by Xe adsorption at 60 K and desorption during warming to 300 K. Calibration experiments indicated that Xe was desorbed by ~90 K, in agreement with results for Ag(111), where multilayers were found to desorb at ~70 K and the first layer at ~90 K.[12,14] Substrate Ga and As 3*d* core-level EDC's taken before and after this process differed only in the Gaussian width of the surface and bulk features, i.e., phonon broadening. Most importantly, the binding energy of the substrate core levels changed by less than 30 meV. This shift is consistent with the temperature-dependent position of E_F in the semiconductor gap (EDC's for the clean surface were collected at 60 K and those following Xe desorption were generally collected at 300 K). We conclude that the Xe adsorption-desorption process did not induce band-bending changes or structural modification of the GaAs(110) surface.

Metal-cluster morphologies on Xe and on GaAs(110)

In Fig. 2 we show the rate of attenuation of Xe 4*d* emission from 30-Å-thick buffer layers as a function of nominal metal coverage. Results are displayed for Ag, Al, Au, Co, Ga, and Ti. The emission from the Xe layer was normalized to the value for zero metal coverage, taking the total Xe 4*d* emission for 200 L on GaAs as unity. As can be seen, there is initial attenuation for all metals. In particular, the Xe emission is reduced to ~70% of its starting value for coverages below 1 Å, and it is likely that the surface is covered by small metal clusters. For metal coverages exceeding ~5 Å, attenuation is virtually constant, demonstrating that areas of the Xe surface remain exposed. The absence of significant deviations in the attenuation for all six metals indicates that the nucleation and growth of the clusters on the interlayer is largely metal independent.

Clusters are brought into contact with the GaAs(110) surface when the Xe buffer layer is desorbed. In Fig. 2 we compare the attenuation results for clusters on Xe to those for clusters on GaAs. In the latter case, the Ga and As 3*d* emission from the clean cleaved surface is taken as unity. If Xe desorption does not produce any morphology changes, then the attenuation results should be indistinguishable. Indeed, the two curves are indistinguishable below ~10 Å for the six different metals. We conclude that, as for the Xe interlayer, the GaAs(110) surface is covered by small metal clusters below 1 Å and by larger clusters between 1 and 10 Å, leaving large areas of substrate exposed. Above ~10 Å the metal clusters attenuate emission from GaAs much more rapidly than emission from the Xe interlayer. This suggests that there are structural changes when the clusters reach the semiconductor. Such sintering and wetting of the surface results in a more complete coverage of the surface. These effects are likely to occur at lower coverage as well, but they cannot be identified with photoemission attenuation results.

A crude estimate of the size of the clusters can be obtained by assuming them to be uniform hemispheres distributed across the surface. In this case, the normalized substrate emission (either Xe or GaAs) can be written

$$\frac{I(\Theta)}{I(0)}=1-\frac{3\Theta}{2R}\left\{1+\frac{2}{R^2}\left[\lambda(R+\lambda)\exp\left[-\frac{R}{\lambda}\right]-\lambda^2\right]\right\},$$

where λ is the photoelectron mean free path, R is the cluster radius, and Θ the amount of metal deposited in Å. From the data in Fig. 2, we find $R\cong 10$ Å for $\Theta=1$ Å, corresponding to ~100 atoms in the cluster. For deposition between 5 and 15 Å on Xe, R varies between 30 and 40 Å (3000–6000 atoms per hemisphere). This large estimated cluster size is consistent with the high mobility of metal atoms on Xe surfaces where there are only weak metal-Xe interactions. The fact that the measured attenuation rate between 5 and 15 Å is slow suggests that the number of clusters is essentially the same as at lower coverages and that most of the deposited atoms become incorporated in those large clusters.

We speculate that the nearly constant Xe attenuation for coverages higher than 15 Å implies that some of the metal clusters are embedded in the Xe layer or that small amounts of Xe cover the clusters. Xe displacement would not be surprising, given the relative heats of formation for Xe and any of these metals. Likewise, the presence of Xe on the clusters is consistent with the very broad Xe 4*d* emission observed upon cluster formation. Such broadening reflects spatial inhomogeneities in the work function of the surface, consistent with metal-cluster formation and Xe adsorption. It is also possible that some cluster sintering occurs within the Xe layer, thereby providing another explanation for the increased GaAs attenuation relative to that for Xe at higher metal coverages. Although the detailed morphology of the cluster/Xe interface is not known completely, the conclusions of this paper do not depend on detailed knowledge of those interfaces. It suffices to note that the buffer layer prevents isolated metal atoms from inducing GaAs surface disruption.

To gain further information regarding the structure and morphology of the metal-cluster/GaAs(110) interface, scanning- and transmission-electron-microscopy studies were undertaken. In the upper portion of Fig. 3 we show results for 7 Å Au(cluster)/GaAs(110). As can be seen, by 7 Å there has been considerable sintering and network formation, but large portions of the surface are exposed. Direct evidence for sintering of several clusters can be seen in Fig. 3(a) in a plan-view TEM micrograph. The size of the large central aggregate is approximately 1000 Å. In Fig. 3(b) we show a transmission electron micrograph of a cross section through the Au cluster/GaAs interface. For this section, the lateral spacing between clusters along the [110] direction is 200–250 Å, and there is intimate contact between the clusters and the substrate. Figure 3(c) shows a high-resolution lattice image of one of the clusters. Inspection of the left portion of this cluster shows lattice images of (111) Au planes separated by 2.5 Å. The region at the right side of this cluster also appears to well defined, but the orientation of the Au(111) planes is different. This indicates that one Au cluster consists of several grains of Au. From this image we can see an abrupt interface without preferential lattice orientation between the metal cluster and the semiconductor surface. The thickness of the clusters is ~60 Å. There is

no evidence for reaction between Au and the GaAs substrate. The reason for the slightly fuzzy image in the central part of the metal cluster close to the substrate (indicated by arrow) is probably related to differently oriented small grains (or distortion at the grain boundary) where lattice spacing between planes is smaller than the resolution of the microscope (below 1.4 Å).

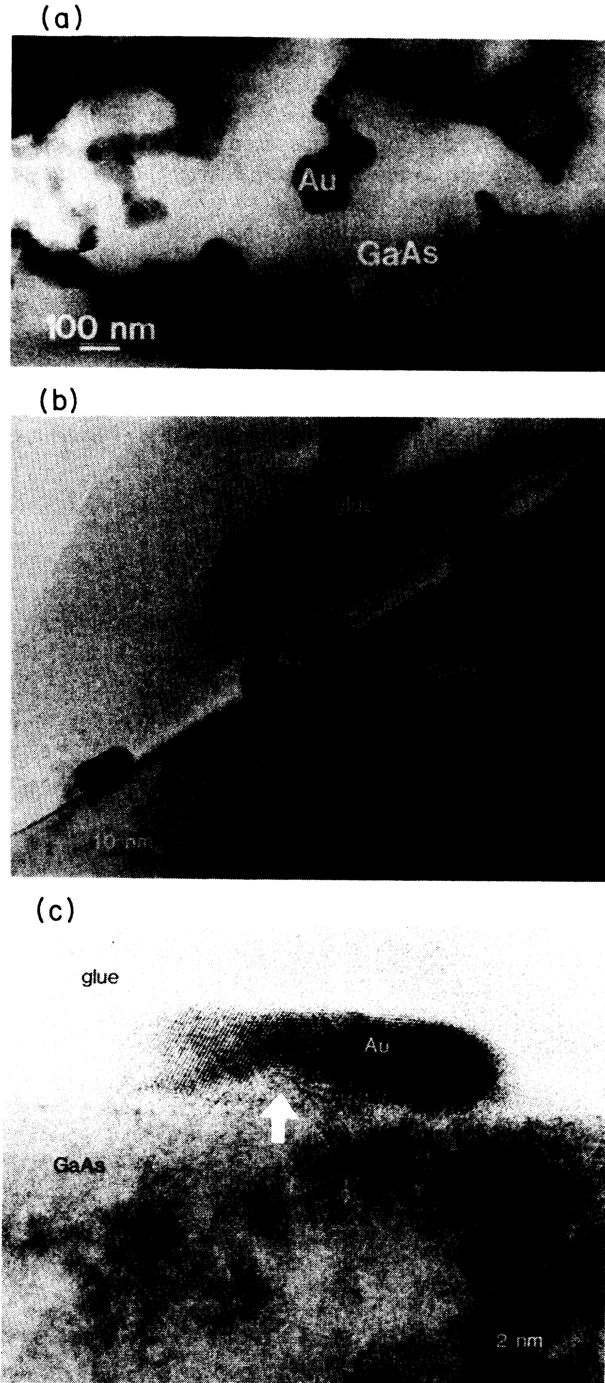

FIG. 3. Upper panel shows a plan view of the 7 Å Au(cluster)/GaAs interface with interconnected metallic clusters. Center panel shows several clusters in cross section. Bottom panel shows high-resolution images which reveal good contact to the GaAs surface and evidence for sintering of two or more microcrystallites of Au.

Valence-band evolution for cluster and atom deposition

From the above it is clear that the metal aggregates formed by cluster deposition onto GaAs(110) are rather extended, even for 7 Å nominal coverage. In order to investigate the onset of metallic character, we have studied the valence-band evolution for clusters corresponding to depositions between 0.1 and 34 Å. Representative results are shown at the right of Fig. 4 for Ti clusters and at the right of Fig. 5 for Ag clusters, with energies referenced to the Fermi level, E_F. For comparison, the left side of each figure shows results obtained by conventional atom deposition. For 0.05 Å atom deposition onto n-type GaAs at 60 K, the Ti d-derived states appear in the gap centered ~1 eV below E_F. For 0.5- and 1-Å Ti–atom deposition at 60 K, the overlayer is still below the metallization threshold, and there is no emission at E_F. Between 1 and 2 Å, however, the metallization threshold is exceeded, and d-band emission at E_F is observed. Broadening of the d-band emission also occurs and, by 16-Å deposition the overlayer is fully metallic. In contrast, cluster deposition of 1 Å gives rise to a metallic Fermi-level cutoff.

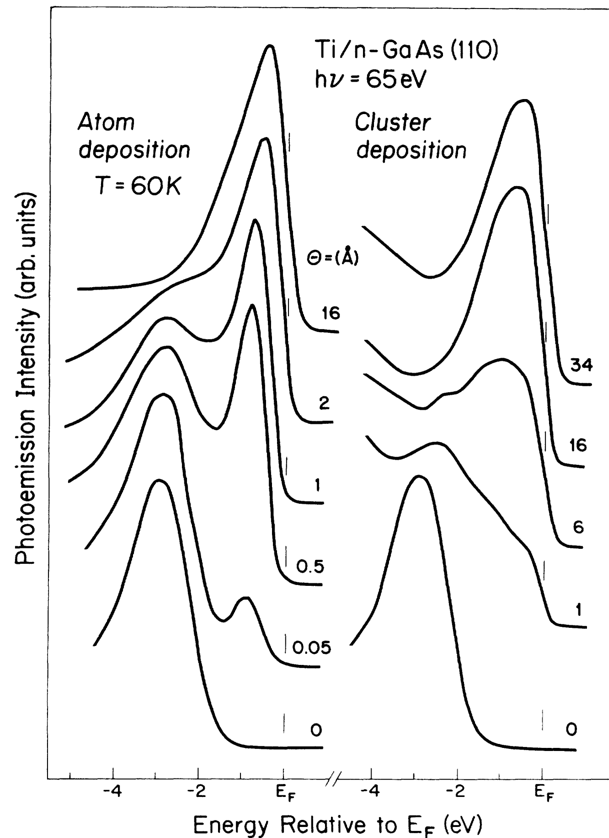

FIG. 4. Representative valence-band spectra for Ti-cluster deposition (right) and Ti-atom deposition at 60 K (left). For atom deposition, the Ti d levels initially appear ~1 eV below E_F, and the Fermi edge does not fully develop until $\Theta \geq 2$ Å. For cluster deposition, the Ti-derived features are less distinct because of the relatively strong contribution from the exposed GaAs substrate, but the Fermi edge is clearly present for $\Theta = 1$ Å. This verifies the metallic nature of the clusters.

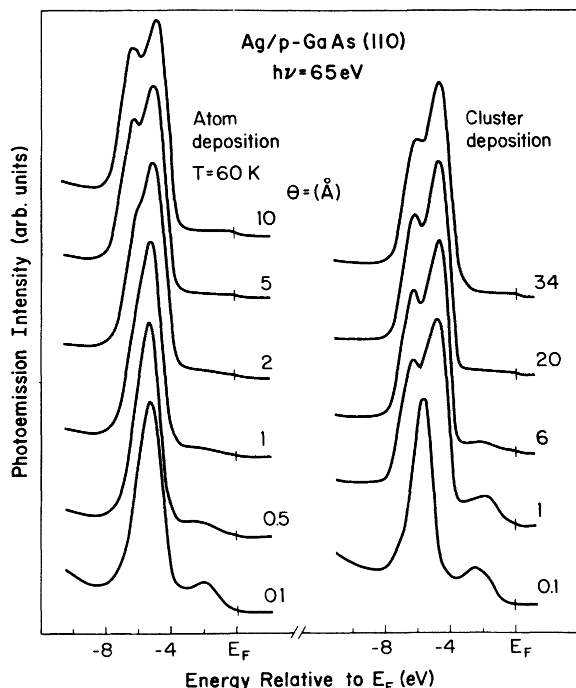

FIG. 5. Representative valence-band spectra for Ag-cluster deposition (right) and Ag-atom deposition at 60 K (left). For atom deposition, the Ag d bands gradually broaden to their full metallic width by $\Theta \sim 5$ Å. For cluster deposition, this width is already achieved by $\Theta = 1$ Å. This demonstrates, similar to Fig. 4, the metallic character of the clusters even for relatively small coverages.

This is expected because the attenuation measurements indicate that the clusters are 10 Å in radius (~ 100 atoms), and such a cluster should be metallic. The very different line shapes for 1-Å cluster and 1-Å atom deposition demonstrate that the clusters cover a relatively small portion of the surface and emission from the GaAs substrate is still strong. In contrast, atom deposition leads to a more uniform coverage of the GaAs surface, and substrate emission is much lower for like metal coverages. At higher coverage the spectra are more similar to those for atom deposition because almost all of the surface is covered by Ti clusters and the substrate emission is strongly attenuated.

Examination of the changing Ag d-band width for Ag cluster and atom deposition onto GaAs(110) makes it straightforward to follow the developing overlayer metallicity. For atom deposition at 60 K, the full width at half maximum (FWHM) increases gradually until it reaches its fully metallic value at ~ 5 Å.[15] In contrast, the Ag d-band emission for 1 Å cluster deposition exhibits fully metallic width and shape. Close inspection of the emission near E_F shows a distinct metallic cutoff for all cluster coverages ≥ 1 Å. The step is difficult to see in Fig. 5 because of the much stronger d-band emission relative to the sp states at E_F, but it is clear when the scale is expanded. In contrast, a metallic Fermi edge is not observed for atom deposition until $\Theta \geq 5$ Å. All of these results indicate that the cluster-deposition technique produces metallic clusters, even for $\Theta = 1$ Å.

Core-level line shapes

In order to determine the morphology of the contacts between clusters and semiconductor surfaces, we have examined the Ga and As $3d$ core-level emission as a function of deposition. For direct comparison, we have also examined the effects of atom deposition at 60 and 300 K. Figure 6 compares As $3d$ EDC's taken at $h\nu = 90$ eV for Co-cluster and -atom deposition (photoelectron mean free path ~ 4 Å). These core-level spectra, and those presented in Fig. 7, have been background subtracted and normalized to constant height to emphasize line-shape changes. Aligning spectra with respect to the feature corresponding to emission from bulk As (labeled 1) corrects for surface Fermi-level changes.

The clean cleaved spectra of Fig. 6 were collected at 60 K, but the spectra following cluster deposition and Xe desorption were collected at temperatures between 100 and 300 K. While this made it possible to investigate the temperature stability of the interface, it introduced

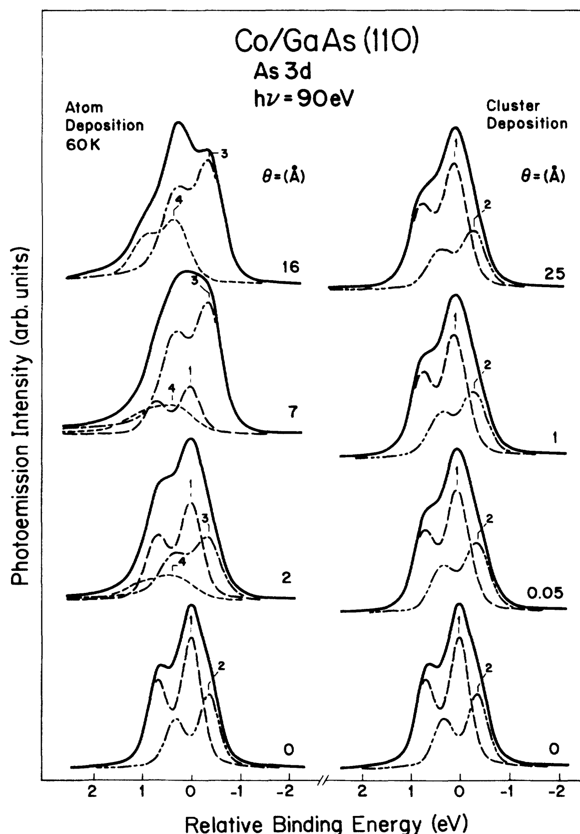

FIG. 6. Representative As $3d$ core-level EDC's and line-shape decompositions for Co-cluster deposition and for Co-atom deposition at 60 K. Components 1 and 2 correspond to emission from bulk and surface As atoms. Components 3 and 4 are induced by atom deposition at 60 K and correspond to As atoms released from the substrate. Cluster deposition alters the relative intensity of the surface and bulk components but introduces no new spectral features.

changes in the core-level line shapes associated with thermal broadening. These changes are reflected in the increase in Gaussian width for the core-level spectra following cluster deposition shown in Fig. 6. These spectra reveal a decrease in the emission intensity from surface atoms (feature 2) relative to that from bulk atoms (feature 1) as the nominal coverage is increased. Most important, *no new adsorbate-induced features* are required to fit the core-level spectra. The stability of these interfaces was demonstrated by the absence of any band bending or line-shape changes while warming to 300 K over a period of ~3 h.

In contrast to the cluster-deposition results, examination of the As core-level spectra for atom deposition at 60 K shows two Co-induced features that dominate for $\Theta \geq 2$ Å; components 3 and 4 correspond to emission from As atoms released from the substrate and bound in different chemical environments at the interface. Similar line-shape changes were found for atom deposition at 300 K.[9] Analysis indicates disruption of ~1–2 monolayers (ML) of the substrate at both temperatures. At 60 K, rapid attenuation of the emission from the disrupted atoms indicate that they are kinetically trapped near the interface, while at 300 K continued emission from these atoms for $\Theta \geq 50$ Å demonstrates segregation to the free surface.[9] We conclude that temperature does not affect the disruption process itself, but rather alters the redistribution of released substrate atoms in the evolving overlayer.

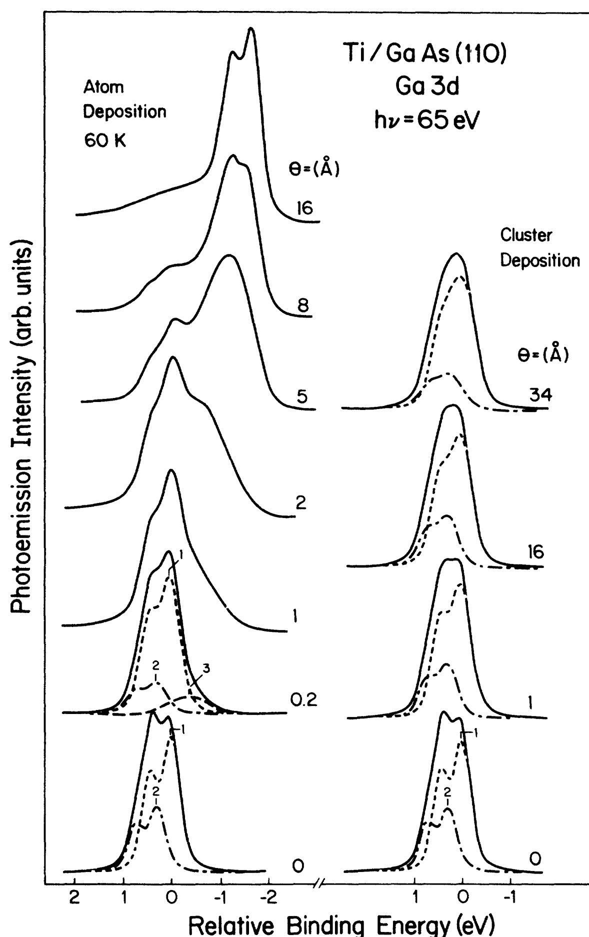

FIG. 7. Representative Ga 3*d* core-level EDC's and line-shape decompositions for Ti-cluster deposition and for Ti-atom deposition at 60 K. Component 3 results from emission from intermixed Ga atoms produced by atom deposition. This component is broad for intermediate coverages because a variety of inequivalent Ga-bonding configurations are present at the interfaces, but it sharpens at higher coverage as Ga bonding becomes more homogeneous. Note that there are no Ti-induced features in the spectra for cluster deposition. Line-shape broadening at higher coverage is a result of possible structural inhomogeneities.

In Fig. 7 we show Ga 3*d* core-level EDC's following Ti-cluster and atom deposition. For atom deposition at 60 K, substantial changes in the Ga 3*d* line shape occur as the Ti coverage increases. Substrate disruption is observed from the lowest coverage and is evident as a rather broad Ti-induced feature (labeled 3) for $\Theta = 0.2$ Å. As feature 3 grows, the intensity of the surface component (labeled 2) decreases rapidly, indicating release of the Ga atoms from surface-bonding configurations into the evolving interface. The large width of feature 3 for $\Theta \leq 8$ Å indicates a variety of inequivalent chemical environments for these released Ga atoms. It sharpens for $\Theta \geq 10$ Å as the environment of the Ga atoms in the Ti overlayer becomes more uniform. As discussed in detail elsewhere,[16] Ti-atom deposition on GaAs(110) disrupts ~3 ML of the substrate at both 60 and 300 K. As for Co/GaAs, there is kinetic trapping of the released substrate atoms near the interface at low temperature.

Inspection of the results of Fig. 7 for Ti cluster deposition shows that there is no evidence for Ti-cluster-induced features in the Ga 3*d* EDC's. Indeed, the only changes following cluster deposition reflect an increase in phonon broadening and a decrease in the relative intensity of emission from surface-shifted Ga atoms compared to bulk Ga atoms. Due to the large size of the clusters compared to the photoemission probe depth (~80 Å cluster thickness versus ~10–20 Å probe depth), we cannot exclude the possibility of metal-substrate interaction beneath the clusters. As we will discuss shortly, the very different Fermi-level positions for cluster and atom deposition on *n*-type GaAs(110) suggest that different mechanisms determine E_F position for the two deposition techniques. Any deviation from the cluster-characteristic E_F position that occurs following cluster deposition can be taken as an indication of metal-substrate interaction caused either by the increase in system temperature or by the inherent instability of the particular metal cluster with respect to metal-GaAs interaction.

From the Co- and Ti-overlayer results in Figs. 6 and 7, we can conclude that there are significant differences in the core-level line shapes for interfaces formed by atom and cluster deposition. The most prominent difference is the absence of any reaction-induced features in EDC's following cluster deposition. Additional studies with Al, Ag, Au, and Ga clusters show that the only line-shape changes observed in both the As 3*d* and Ga 3*d* EDC's involve phonon broadening and the decrease in the surface to bulk (I_S/I_B) emission intensity ratio as the nominal

cluster coverage is increased. The absence of cluster-induced features suggests that this new deposition process is not disruptive and produces abrupt junctions. In contrast, there are radical line-shape changes following atom deposition of Al,[17] Au,[18] Co,[9] Ga,[19] and Ti (Ref. 16) on GaAs(110), and various amounts of substrate disruption, atomic intermixing, reaction, and clustering are revealed by careful line-shape analysis.

It is particularly instructive to consider differences between Ag-cluster and -atom deposition. For atom deposition, clustering occurs spontaneously at 300 K,[9,15] while deposition at 60 K leads to more uniform surface coverage,[9] with weak substrate interaction in both cases. Analysis of the core-level spectra shows distinctly different I_S/I_B ratios for atom deposition at 60 and 300 K, and for direct Ag-cluster deposition. For 300-K atom deposition, the ratio remains equal to the clean-surface value of ~ 0.5 even at $\Theta = 20$ Å, corresponding to $\sim 60\%$ surface coverage. This indicates that the exposed portions of the substrate are largely unperturbed by the Ag clusters. In contrast, atom deposition at 60 K leads to complete loss of emission from the surface-shifted atoms for $\Theta \geq 2$ Å as the uniform overlayer forms and the surface atoms interact with the Ag overlayer. For preformed cluster deposition, I_S/I_B decreases gradually with increasing coverage. This indicates that the clusters modify the surface structure in the region surrounding them and thereby induce the loss of the surface component. We shall return to this shortly in discussions involving Schottky-barrier formation since this process affects Fermi-level movement at the surface.

We have shown that cluster deposition produces abrupt interfaces with no observable substrate disruption, even for reactive metals. We expect that the presence of a metal overlayer does lead to partial or complete surface unrelaxation beneath the clusters, but this area cannot be probed by photoemission. The results discussed in the following section suggest that there is, in general, no surface disruption beneath the clusters, and we conclude that these interfaces are, in a morphological sense, nearly "ideal" or abrupt. Note, however, that the electron-microscopy studies show that epitaxy should not be presumed.

Band bending and surface Fermi-level movement

One of the remarkable properties of interfaces formed by cluster deposition is that the Fermi-level position in the gap is almost independent of the amount of metal deposited. To demonstrate this, we show in Fig. 8 the position of E_F in the gap as a function of metal coverage for Ag, Al, Au, Co, Ga, and Ti clusters deposited onto n-type GaAs(110) doped at 1×10^{17} cm^3. Each point was obtained from a complete cluster-deposition experiment, i.e., obtaining a new GaAs(110) surface by cleaving, determining that E_F was within 60 meV of the CBM (unpinned), condensing a 30-Å Xe buffer layer, depositing the metal onto the buffer layer, desorbing the Xe, and, finally, measuring the Fermi-level movement by analysis of changes in the Ga and As core-level energies using two

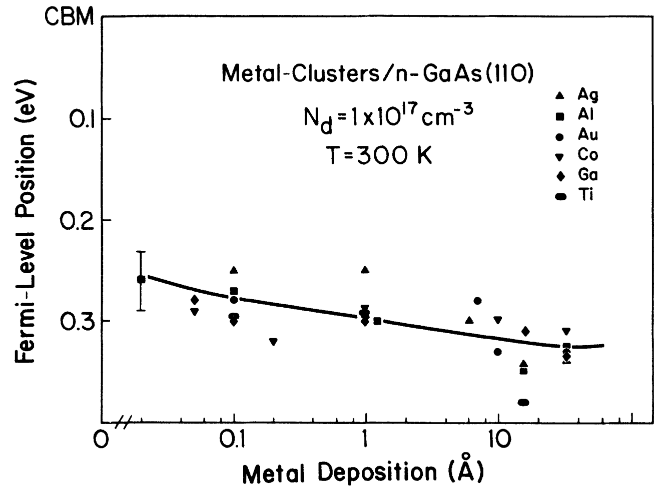

FIG. 8. Fermi-level position as a functional of metal-cluster deposition on lightly doped n-type GaAs(110). The energy positions are almost independent of metal and coverage with a very gradual shift to a position ~ 0.32 eV below the CBM. The average error bar corresponds to ± 0.03 eV. We emphasize that the scatter in data points for the six different metals is remarkably small compared to the measurement accuracy. These values are independent of temperature, except for Ti, which, as discussed in the text, reacts spontaneously. Each point corresponds to a complete experiment beginning with a fresh cleave. For the clean surface, E_F fell within 60 meV of the CBM.

photon energies for each core level. As shown, E_F moved to a position ~ 260 meV below the CBM for 0.02-Å cluster deposition and then gradually moved to ~ 320 meV below the CBM by 35 Å. From Fig. 2 we know that $\sim 90\%$ of the substrate is covered by metal clusters after 30–40 Å, and we expect no E_F movement at higher Θ.

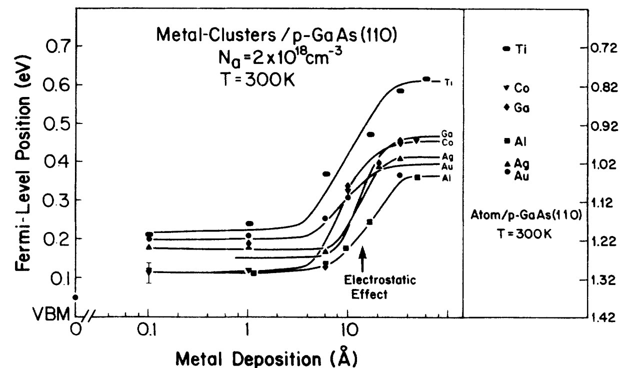

FIG. 9. Fermi-level position as a function of metal-cluster deposition on heavily doped p-type GaAs(110). In all cases, there is an initially flat region 100–200 meV above the VBM and then a step toward midgap at higher coverage as the cluster spacing becomes sufficient to guarantee homogeneous surface potentials. The final Fermi-level position depends on the metal and ranges from 0.37 eV above the VBM for Al to 0.62 eV above for Ti. A typical error bar is shown on the left. Each point corresponds to a complete experiment beginning with a fresh cleave. For comparison, we show at the right of the figure the E_F positions obtained by atom deposition. The final positions are close for Au and Ag, but differ significantly for the other metals.

We emphasize that E_F moved by only ~ 60 meV over 3 orders of magnitude of metal coverage, and that the changes are entirely metal independent based on approximately 30 cluster experiments summarized in Fig. 8. Such coverage independence and lack of metal specificity has not been found in atom-deposition experiments and cannot be described with existing models of Schottky-barrier formation. Likewise, the position of E_F high in the gap is contrary to that expected for pinning positions associated with deep levels or defects, or metal-induced gap states.

In Fig. 9 we show the very different evolution of the surface Fermi level for metal-cluster deposition on p-type GaAs(110) doped at 2×10^{18} cm^{-3}. The results show the movement to 100–200 meV above the VBM by 0.1 Å, essentially no change until 6–8 Å, where E_F rises to its final position in the gap. For p-type GaAs, the Fermi-level evolution is somewhat metal dependent with energies ranging from ~ 370 meV above the VBM for Al to ~ 650 meV above the VBM for Ti after 25–30 Å deposition. It is noteworthy that the ordering observed at low coverage (Ti, Au, Ag, Al, and Co) is not the same as that at high coverage (Ti, Ga, Co, Ag, and Al), so that the step height is also metal specific.

The very obvious difference between the results of Figs. 8 and 9 is the step for p-type GaAs which occurs at 6–8 Å. We note that the p-type GaAs samples were doped at 2×10^{18} cm^{-3}, while the n-type GaAs samples were doped at 1×10^{17} cm^{-3}. Thus the step is due to the coverage-related changes in cluster separation, with the final E_F position achieved when cluster spacing becomes comparable to, and ultimately less than, the substrate-depletion width. This transition from isolated clusters on a largely unexposed surface to clusters that are close enough to produce uniform surface pinning occurs near ~ 10 Å. For 0.4-eV band bending corresponding to an average final E_F position in Fig. 9, the depletion width is 170 Å for $N=2\times10^{18}$ cm^{-3} and 760 Å for $N=1\times10^{17}$ cm^{-3}. The simple hemispherical model described above gives an estimate of $R=30$ Å for $\Theta=6$ Å, so that the spacing between uniformly distributed clusters would be ~ 40 Å. Plan-view transmission-electron-microscopy (TEM) results for 7-Å Au clusters [Fig. 3(a)] show that clusters are not distributed uniformly. The cross-sectional view along the [110] direction [Fig. 3(b)] shows an average island separation of ~ 250 Å. The fact that a step is observed in every case points to common morphological evolution of the clusters on the surface (consistent with the attenuation results of Fig. 2) and equivalent modification of the surface electrostatics. The low-coverage regime then corresponds to dispersed clusters on both n- and p-type GaAs, but the shorter depletion width for the more heavily doped p-type samples requires higher nominal coverages to realize uniform surface pinning by the clusters.

To prove that the step near 10 Å depends on the bulk dopant concentration and is electrostatic in origin, we investigated Ag-metal-cluster deposition on p-type GaAs doped at 1×10^{17} cm^{-3}, i.e., the same dopant concentration as that for the n-type samples of Fig. 8. In Fig. 10 we compare the movement of E_F for Ag (clusters) on lightly doped and more heavily doped p-type GaAs. For the lightly doped samples, E_F moved substantially into the gap for 0.02 Å of Ag deposition, and it moved only gradually for higher depositions. The step seen for the higher doped samples was not observed. This confirms that the change from the low-coverage region to the final E_F position for the higher doped samples is electrostatic in origin. We conclude that the gradual changes for lightly doped n- and p-type GaAs are a consequence of the cluster spacing being slightly greater than the depletion width. The Fermi-level position measured above the step for p-type GaAs should then be taken as representative of the average surface effect of the metal clusters.

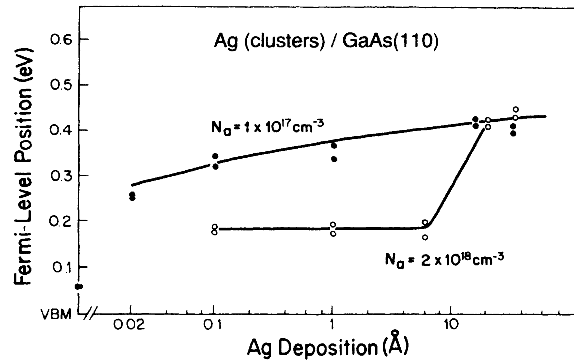

FIG. 10. Fermi-level position for Ag-cluster deposition on p-type GaAs(110) doped at 2×10^{18} and 1×10^{17} cm^{-3}. The step toward midgap at ~ 10 Å shown in Fig. 9 appears for the more heavily doped samples because of surface electrostatics, i.e., the cluster spacing becomes comparable to the depletion width at ~ 10 Å. For the more lightly doped samples, the Fermi-level position is almost coverage independent, as was observed for cluster deposition on like-doped n-type GaAs(110) samples, because the cluster spacing is comparable to the much larger depletion width.

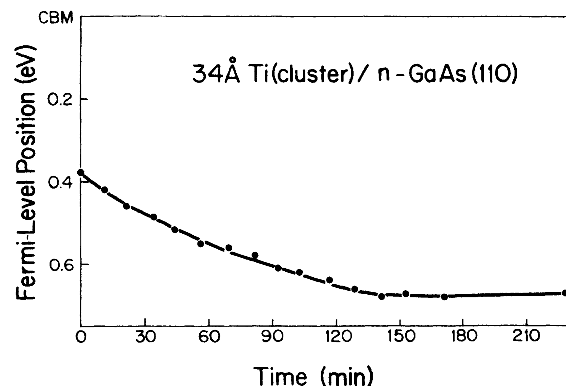

FIG. 11. Fermi-level evolution as a function of time for [34 Å Ti(cluster)]/[n-type GaAs(110)]. Spontaneous interface reaction between the clusters and the substrate is believed to be responsible for the observed changes in E_F. The final E_F position agrees with that found for conventional atom deposition. This temperature dependence was observed only for extremely reactive Ti clusters.

In the discussion above we concluded that cluster deposition produced stable interfaces for the weakly reactive metals as well as for Co and Al. This conclusion is supported by following the movement of E_F in the gap as the cluster/GaAs interfaces are warmed from ~ 100 to 300 K. These studies found the E_F position to be independent of temperature for Al, Ga, Co, Ag, and Au, provided account is taken of the slight temperature dependence of the position of E_F and the value of the band gap of GaAs. For highly reactive Ti, however, reaction was not completely suppressed upon warming, and investigations of E_F movement showed temperature dependence. The results of Figs. 8 and 9 give the Fermi-level position for Ti cluster deposition for the lowest temperature measured, but E_F moved toward midgap as the temperature was increased to 300 K. This trend is shown in Fig. 11 for (34 Å Ti)/(n-type GaAs). Immediately following Xe desorption at ~ 100 K, E_F was 0.38 eV below the CBM, corresponding to the $t=0$ point of Fig. 11. After ~ 120 min, E_F had reached its final position 0.67 eV below the CBM. This final position is in good agreement with the value observed for atom deposition.[16] Warming experiments for p-type GaAs at high coverage showed no change because the final E_F position for cluster and atom deposition is the same. At lower coverage, warming of an interface formed with 0.2 Å Ti on the highly doped p-type GaAs of Fig. 9 showed no change in E_F since the clusters were widely separated and reaction beneath them would not alter E_F across the uncovered surface. During these warming experiments, the changes that were observed in the Ga and As core levels can be attributed to phonon broadening. As previously noted, due to the movement of E_F during warming we infer that Ti cluster is so unstable when in contact with GaAs that thermodynamically driven reaction takes place despite kinetic constraints. Some reaction by ~ 100 K cannot be excluded. Since E_F remained far from midgap for temperatures up to 300 K for the other metal clusters, we conclude that those interface regions are free of disruptive metal-substrate interaction. Studies of these interfaces using electron microscopy are presently underway.

In Table I we compare the highest-coverage E_F positions for cluster deposition for Al, Ag, Au, Co, Ga, and Ti with those for atom deposition at both 60 and 300 K. We stress that these comparisons are based on measurements with the same bulk dopant concentration N since the position of E_F is dependent on N.[10] The energy shifts were obtained by line-shape analysis of the substrate core levels, the necessity of which can be seen from the complex line shapes of Figs. 6 and 7. Table I references all energies to the CBM. When account is taken of the temperature dependence of the band gap of GaAs, we see that the barrier heights for $n-$type GaAs and$p$-type GaAs do not change with teperature. Significantly, the spread in the values for the E_F position for clusters is only 60 meV for n-type GaAs and the barrier height is about half of that for atom deposition. For p-type GaAs, the barrier heights are the same to within 30 meV for atom and cluster deposition for Ag and Au, deviate by less than 100 meV for Al, Ga, and Ti, and by 140 meV for Co. Atom deposition always gives the position farther from the VBM when there is deviation.

Models that address temperature-dependent E_F evolution[6,7,20] divide the behavior into low- and high-coverage regimes because there is a transition from nearly flat bands to near-midgap pinning near 1–2 ML for lightly doped n- and p-type GaAs. The high-coverage regime is particularly interesting in view of the cluster-deposition results because E_F movement toward midgap is believed to be related to the onset of metallicity and wave-function delocalization in the overlayer. It is intriguing, then, that deposition of fully metallic clusters on n-type GaAs results in E_F positions so different from those obtained after metallization by atom deposition. The behavior for n-type GaAs indicates equivalent barrier heights for all stable clusters, implying that the Fermi-energy position is related to the GaAs(110) surface rather than the chemical identity or any other property of the overlying cluster. For clusters on p-type GaAs, E_F is more metal dependent and moves farther into the gap. This asymmetric behavior suggests that these clusters induce electrically active states with more donorlike than acceptorlike character at the surface.

According to the MIGS model, metallic overlayers should pin the Fermi level at the charge-neutrality point in the semiconductor band gap, and this pinning position should show little metal specificity. For GaAs this point is estimated to be 0.7 eV above the VBM.[4] Our results show that none of the final E_F positions are close to this predicted MIGS value for n- or p-type GaAs for cluster deposition. From Table I, the results for cluster deposition on n-type GaAs are far from midgap, while those for p-type GaAs are closer, but exhibit a metal-dependent spread of 260 meV. These facts suggest that MIGS are not present in sufficient density to play an important role in determining the Fermi-level position following cluster deposition.[4]

Another model of Schottky-barrier formation relates pinning to antisite defects created by adatom condensation. Such defects produce distinct pinning positions that are intrinsic to the semiconductor. For cluster deposition, we see that Fermi-level movement is unrelated to adatom-induced defects created in the GaAs. This is reasonable because there is no detectable cluster-induced substrate disruption. We also see that the final E_F positions for atom deposition are inconsistent with energies, 0.52 and 0.75 eV above the VBM, predicted by defect models.[1] It should be noted, however, that substrate disruption and defect formation may occur beneath the clusters and may be unobservable with photoemission. In the presence of the metallic cluster overlayer, a density of defects of $\sim 10^{14}$ cm^{-2} is required for E_F pinning. The deviation of the cluster-pinning positions from those predicted by defect models again suggests that the defect density of the metal cluster/GaAs interface is insufficient to be important in determining the E_F position in the gap.

We propose that cluster deposition leads to surface unrelaxation and, therefore, bond modification around and beneath the clusters. This hypothesis is supported by re-

TABLE I. Fermi-level positions (in eV) for metal-cluster deposition and for metal-atom deposition at 60 and 300 K. Values for cluster deposition are from this study. Values for atom deposition are for the highest coverage reported in Refs. 6, 9, 16, and 17. All energies are referenced to the CBM, E_{CBM}, with error bars of ± 30 meV. If the p-type GaAs results for atom deposition were referenced to the VBM, then the Schottky barrier, $E_F - E_{VBM}$, would also be nearly independent of temperature.

	n-type GaAs(110)			p-type GaAs(110)			
	Cluster deposition	Atom deposition		Cluster deposition	Atom deposition		
Metal		300 K	60 K		300 K	60 K	Ref.
Ag	0.32	0.89	0.89	1.00	1.02	1.12	9
Al	0.33	0.70	0.70	1.05	0.96	1.04	17
Au	0.33	0.90	0.87	1.02	1.04	1.10	this work
Co	0.32	0.67	0.67	0.96	0.82	0.92	9
Ga	0.34	0.60	0.84	0.95	0.87	0.87	6
Ti	0.38	0.73	0.67	0.79	0.72	0.79	16

sults of detailed analysis of the ratio of the surface to bulk core-level intensities, I_S/I_B, for Ga and As atoms. In the discussion of core level lineshapes it was shown that I_S/I_B decreased from the clean-surface value as the cluster coverage increased. Those changes in I_S/I_B are summarized in Table II for the different clusters and are to be expected if the clusters modify the GaAs(110) surface relaxation in the regions around them. The relaxation that is produced by cleaving gives rise to the surface component observed in the clean cleaved spectra, and, as is well known, sweeps the surface states out of the gap. Unrelaxation would reintroduce surface states into the band gap of GaAs. The deposition of thick clusters could also lead to unrelaxation beneath them, but this effect would not be observed because the photoemission signal from these regions is attenuated by the thick metal overlayer. On the other hand, this unrelaxation must extend beyond the cluster perimeter as our photoemission probe does indeed detect changes in I_S/I_B. The loss or partial loss of surface relaxation would result in a large number of intrinsic surface states in the band gap. Calculations of such intrinsic states for unrelaxed GaAs(110) have shown surface levels within ~ 150 meV of the CBM (Ref. 21) and states at ~ 450 meV above the VBM. These states would, of course, be modified by the presence of the metallic clusters. Hence, unrelaxation for p-type GaAs should lead to E_F movement deeper into the gap, while E_F would rémain close to the CBM for unrelaxed n-type GaAs. The fact that the E_F position for n-type GaAs is independent of metal is consistent with this model. The cluster-deposition results on p-type GaAs suggest, however, that there are additional factors affecting the positions of E_F in the gap which are reflected in the spread in final pinning values (260 meV).

It is very interesting that the sensitivity to the nature of metal clusters is lacking from the E_F results on the n-type substrates. A plausible scenario for this behavior would necessarily involve two parallel mechanisms for Schottky-barrier formation at these interfaces. The first and dominant mechanism would be associated with surface unrelaxation and the reintroduction of intrinsic states in the gap. The calculations for these states agree with our results in the sense that the ultimate E_F positions for p-type GaAs lie deeper in the band gap than for the n-type GaAs. Also, the existence of these states in the gap is experimentally supported by recent scanning-tunneling-microscopy (STM) measurements on GaAs(110) covered by Sb islands.[22] The second mechanism is associated with metal-specific modifications of the barrier height on p-type semiconductors, but apparently

TABLE II. Surface to bulk emission intensity ratio, I_S/I_B, for metal-cluster deposition on GaAs(110). Values for Ga 3d (As 3d) core levels were obtained at $h\nu = 65$ (90) eV. Photoelectron mean free paths are ~ 3.5 Å.

Θ (Å)	Ag	Au	Co	Ga	Ti	Al
0	0.51 (0.52)	0.52 (0.52)	0.54 (0.57)	0.54 (0.50)	0.52 (0.56)	0.54 (0.54)
0.1	0.45 (0.47)	0.49 (0.48)		0.48 (0.49)	0.47 (0.48)	
1	0.45 (0.45)	0.42 (0.47)		0.47 (0.48)	0.47 (0.48)	
1.2						0.47 (0.48)
2			0.48 (0.47)			
6	0.44 (0.40)			0.43 (0.42)	0.47 (0.46)	0.48 (0.48)
7		0.44 (0.47)				
10		0.43 (0.47)	0.49 (0.48)	0.42 (0.41)		0.42 (0.39)
16	0.40 (0.40)	0.38 (0.40)		0.43 (0.42)	0.41 (0.43)	0.40 (0.38)
20	0.38 (0.42)	0.38 (0.41)				
25			0.38 (0.42)			
34	0.38 (0.35)	0.40 (0.35)		0.36 (0.39)	0.35 (0.40)	0.35 (0.37)

plays no role for the n-type ones. The precise nature of this mechanism is not currently understood.

It is particularly interesting to further examine the unrelaxation model for Ag/GaAs. As we noted previously, Ag atom deposition at 300 K results in the spontaneous formation of Ag clusters, but no change in I_S/I_B is observed. This suggests that the uncovered substrate is unchanged by the presence of the Ag clusters. We speculate that under these conditions the Ag clusters grow in a manner which allows accommodation of the cluster to the substrate surface structure. Specifically, the sequential deposition of Ag atoms and their migration across the GaAs surface to nucleation sites for cluster growth may allow the Ag atoms to agglomerate without altering the surface structure. In contrast, deposition of large preformed Ag clusters allows no such metal accommodation, and the substrate areas around (and possibly beneath) the clusters are modified by the cluster presence. The similar final morphologies, but quite different final E_F positions (Table I) for Ag/GaAs interfaces formed by these different techniques, represent a clear demonstration of the dependence of band bending upon the structural details of the intimate contacts and the energetics of the cluster-formation process.

CONCLUSIONS

We have established and characterized formation of abrupt, nearly ideal metal/GaAs interfaces by depositing metal atoms on a Xe interlayer and subsequently desorbing the Xe. This procedure produces large, fully metallic clusters on the GaAs surface without any observable substrate dusruption. Interfaces formed in this manner show intriguing E_F evolution that is virtually metal and coverage independent for n-type GaAs, but weakly dependent on the metal for p-type GaAs. The Fermi-level energies are quite distinct from those observed for interfaces formed by direct atom deposition for n-type GaAs, but coincide better for p-type GaAs. We propose that the differences in E_F positions are related predominantly to loss of surface relaxation around the clusters and the creation of new bonding configurations involving the clusters. We see no evidence for a sufficient density of MIGS or conventional defect levels to determine E_F pinning position for preformed metal-cluster deposition. The details of the Fermi-level evolution for these interfaces are not completely understood at this time, but the abrupt disruption-free nature of the interfaces make them particularly attractive for metal-semiconductor-junction modeling. Certainly, our results demonstrate the importance of the energetics associated with atom condensation and bond formation as far as E_F evolution is concerned. Consequently, comparison of results for Ag clusters grown spontaneously on GaAs during 300-K atom deposition and those deposited with the cluster technique shows dramatically different band bending. Finally, we note that the cluster-deposition technique described herein can be extended to other systems, both metallic and nonmetallic.[23]

ACKNOWLEDGMENTS

The studies at the University of Minnesota were supported by the Office of Naval Research under Contracts No. N00014-86-K-0427 and No. N00014-87-K-0029. The photoemission experiments were done at the University of Wisconsin Synchrotron Radiation (Stoughton, WI), a national facility operated by the University of Wisconsin for the National Science Foundation. The assistance of the staff of that laboratory is gratefully acknowledged. M. Schabel, S. J. Severtson, and J. P. Sullivan generously assisted with data acquisition and analysis. The TEM studies were supported by the Office of Naval Research under Contract No. N00014-86-K-0668 and by the U. S. Department of Energy under Contract Nos. DE-AC03-76SF00098 and DE-AC03-76SAF0009. The use of the facilities of the National Center for Electron Microscopy at Lawrence Berkeley Laboratory is gratefully appreciated.

[1]W. E. Spicer, P. W. Chye, P. R. Skeath, C. Y. Su, and I. Lindau, J. Vac. Sci. Technol. **16**, 1427 (1979); W. E. Spicer, Z. Liliental-Weber, E. Weber, N. Newman, T. Kendelewicz, R. Cao, C. McCants, P. Mahowald, K. Miyano, and I. Lindau, J. Vac. Sci. Technol. B **6**, 1245 (1988).

[2]L. J. Brillson, Surf. Sci. Rep. **2**, 123 (1982); J. Vac. Sci. Technol. **16**, 1137 (1978).

[3]J. M. Woodall and J. L. Freeouf, J. Vac. Sci. Technol. **19**, 7984 (1981); J. L. Freeouf and J. M. Woodall, Appl. Phys. Lett. **39**, 727 (1981).

[4]V. Heine, Phys. Rev. **138A**, 1689 (1965); S. G. Louie, J. R. Chelikowsky, and M. L. Cohen, Phys. Rev. B **15**, 2154 (1977); J. Tersoff, Phys. Rev. Lett **52**, 465 (1984); J. Vac. Sci. Technol. B **3**, 1157 (1985).

[5]L. J. Brillson, R. E. Vitturo, C. Mailhiot, J. L. Shaw, N. Tache, J. McKinley, G. Margaritondo, J. M. Woodall, P. D. Kirchner, G. D. Pettit, and S. L. Wright, J. Vac. Sci. Technol. B **6**, 1263 (1988).

[6]K. Stiles, A. Kahn, D. G. Kilday, and G. Margaritondo, J. Vac. Sci. Technol. B **5**, 987 (1987); K. Stiles and A. Khan, Phys. Rev. Lett. **60**, 440 (1988); J. Vac. Sci. Technol. B **6**, 1392 (1988).

[7]K. K. Chin, T. Kendelewicz, C. McCants, R. Cao, K. Miyano, I. Lindau, and W. E. Spicer, J. Vac. Sci. Technol. A **4**, 969 (1986); R. Cao, K. Miyano, T. Kendelewicz, K. K. Chin, I. Lindau, and W. E. Spicer, J. Vac. Sci. Technol. B **5**, 998 (1987).

[8]G. D. Waddill, C. M. Aldao, I. M. Vitomirov, Y. Gao, and J. H. Weaver, J. Vac. Sci. Technol. A **7**, 865 (1989).

[9]G. D. Waddill, I. M. Vitomirov, C. M. Aldao, and J. H. Weaver, Phys. Rev. Lett. **62**, 1568 (1989); G. D. Waddill, C. M. Aldao, I. M. Vitomirov, S. G. Anderson, C. Capasso, and J. H. Weaver, J. Vac. Sci. Technol. B **7**, 950 (1989).

[10]C. M. Aldao, I. M. Vitomirov, G. D. Waddill, S. G. Anderson, and J. H. Weaver, Phys. Rev. B **41**, 2800 (1990); S. G. Anderson, C. M. Aldao, G. D. Waddill, I. M. Vitomirov, C. Capasso, and J. H. Weaver, Appl. Phys. Lett. **55**, 2547 (1989).

[11]J. J. Joyce, M. del Giudice, and J. H. Weaver, J. Electron.

Spectrosc. Relat. Phenom. **49**, 31 (1989); I. M. Vitomirov, C. M. Aldao, Z. Lin, Y. Gao, B. M. Trafas, and J. H. Weaver, Phys. Rev. B **38**, 10 776 (1988).

[12]For discussions of Xe condensation on metal surfaces, see K. Wandelt, J. Vac. Sci. Technol. A **2**, 802 (1984); S. Raaen and M. Strongin, Phys. Rev. B **32**, 4289 (1985); T.-C. Chiang, G. Kaindl, and T. Mandel, *ibid.* **33**, 695 (1986).

[13]N. Schwenter, Phys. Rev. B **14**, 5490 (1976).

[14]R. J. Behm, C. R. Brundle, and K. Wandelt, J. Chem. Phys. **85**, 1061 (1986).

[15]R. Ludeke, T.-C. Chiang, and D. E. Eastman, J. Vac. Sci. Technol. **21**, 599 (1982); K. K. Chin, S. H. Pan, D. Mo, P. Mahowald, N. Newman, I. Lindau, and W. E. Spicer, Phys. Rev. B **32**, 918 (1985).

[16]C. M. Aldao, G. D. Waddill, S. G. Anderson, and J. H. Weaver, Phys. Rev. B **40**, 2932 (1989); I. M. Vitomirov, G. D. Waddill, C. M. Aldao, Steven G. Anderson, C. Capasso, and J. H. Weaver, *ibid.* **40**, 3483 (1989); M. W. Ruckman, M. del Giudice, J. J. Joyce, and J. H. Weaver, *ibid.* **33**, 2191 (1986); D. M. Hill, F. Xu, Z. Lin, and J. H. Weaver, *ibid.* **38**, 1893 (1988).

[17]S. G. Anderson, C. M. Aldao, G. D. Waddill, I. M. Vitomirov, S. J. Severtson, and J. H. Weaver, Phys. Rev. B **40**, 8305 (1989).

[18]W. G. Petro, T. Kendelewicz, I. Lindau, and W. E. Spicer, Phys. Rev. B **34**, 7089 (1986).

[19]P. Skeath, I. Lindau, C. Y. Su, and W. E. Spicer, Phys. Rev. B **28**, 7051 (1983); P. Skeath, I. Lindau, P. W. Chye, C. Y. Su, and W. E. Spicer, J. Vac. Sci. Technol. **16**, 1143 (1979); P. Skeath, C. Y. Su, I. Lindau, and W. E. Spicer, *ibid.* **17**, 874 (1980).

[20]W. Mönch, J. Vac. Technol. B **6**, 1270 (1988).

[21]D. J. Chadi, Phys. Rev. B **18**, 1800 (1978).

[22]R. M. Feenstra and P. Mårtensson, Phys. Rev. Lett. **61**, 447 (1988).

[23]C. M. Aldao, G. D. Waddill, I. M. Vitomirov, and J. H. Weaver, J. Vac. Sci. Technol. A **7**, 817 (1989).

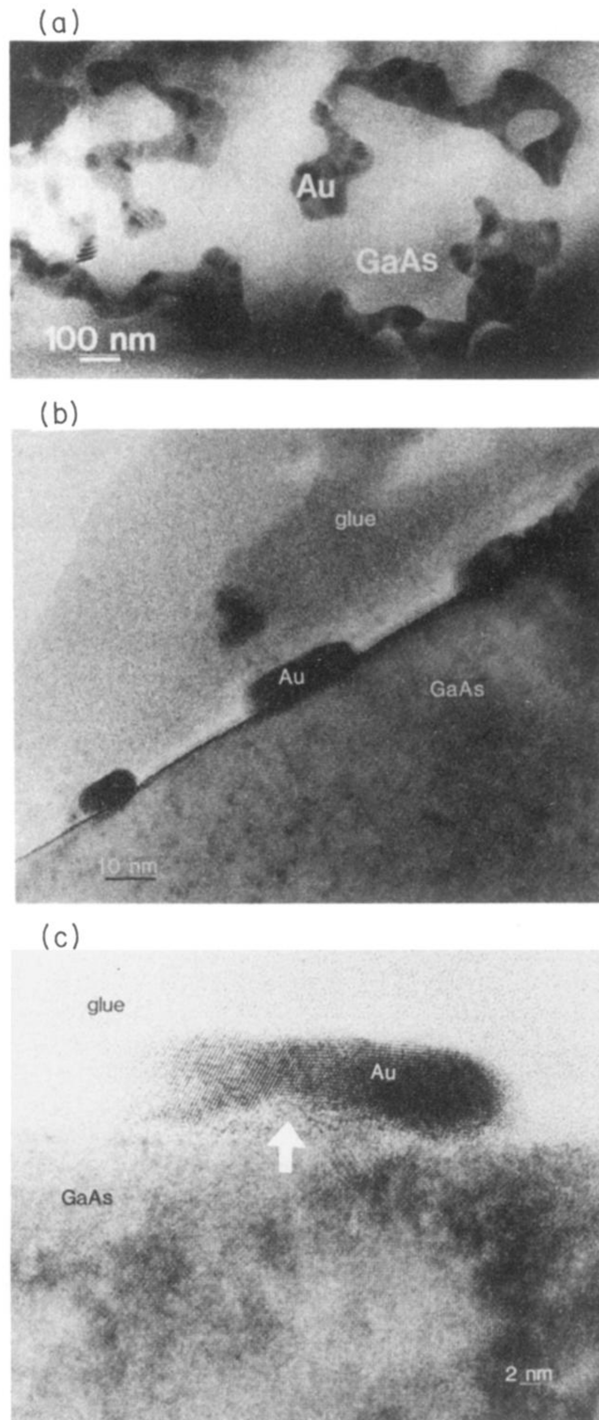

FIG. 3. Upper panel shows a plan view of the 7 Å Au(cluster)/GaAs interface with interconnected metallic clusters. Center panel shows several clusters in cross section. Bottom panel shows high-resolution images which reveal good contact to the GaAs surface and evidence for sintering of two or more microcrystallites of Au.